Electronic supplemental information

Reduction and oxidation of Au adatoms on the CeO_2(111) surface—DFT+U versus hybrid functionals

Christopher Penschke and Joachim Paier*

Institut für Chemie, Humboldt-Universität zu Berlin, Unter den Linden 6, 10099 Berlin, Germany

1. TPSSh atomization energies: Comparison VASP -- Turbomole

Molecular atomization energies calculated using VASP 5.2.12 employ supercells of $10 \times 11 \times 12$ Å^3. The plane-wave cutoff was set to 1000 eV and the PBE PAW pseudopotentials released as of VASP 5.2 were employed. The atomic positions were relaxed until the forces acting on the atoms were less than 0.01 eV/Å. Spurious dipol interactions of replicated images are corrected by the method of Makov and Payne.[1] Structure optimizations using Turbomole 6.5 use the def2-QZVPP local basis set and the quadrature for integration of the xc contributions used multiple grid M5. The structures were optimized employing energy and gradient thresholds of 0.1×10^{-5} and 0.1×10^{-2} atomic units, respectively.

Table S1 TPSSh total energies obtained using VASP (eV) and Turbomole (E_H), as well as therefrom calculated atomization energies (kJ/mol).

	TPSSh Total energies		**Atomization energies**	
Molecules	**VASP [eV]**	**TM [E_H]**	**VASP [kJ/mol]**	**TM [kJ/mol]**
H_2	-7.5709	-1.1799	-470.9	-471.5
LiF	-12.7939	-107.4708	-551.6	-555.5
CO	-20.1643	-113.3651	-1046.0	-1046.0
HCO	-22.7276	-113.9102	-1163.5	-1164.0
CH_3OH	-36.8744	-115.7829	-2139.0	-2141.3
H_2CO	-28.1265	-114.5598	-1554.6	-1556.4
H_2O	-17.9490	-76.4643	-947.1	-947.6
O_2	-16.0993	-150.3979	-503.2	-503.3
NH_3	-23.2200	-56.5877	-1246.0	-1246.4
PH_3	-21.8626	-343.1863	-1039.1	-1039.2
CH_2 (triplet)	-15.1798	-39.1802	-830.5	-830.5
Si_2H_6	-42.8421	-582.6626	-2295.2	-2298.5
ClO	-14.3945	-535.3872	-282.5	-279.8
ClF	-12.8680	-560.0484	-262.9	-261.8
C_2H_4	-37.6899	-78.6303	-2368.3	-2369.5
HCN	-24.8930	-93.4684	-1292.5	-1292.1
SO_2	-28.3568	-548.7451	-1048.5	-1041.8
Si_2	-14.2131	-578.9049	-311.7	-311.7
H_2S	-17.3064	-399.4364	-772.9	-772.0
CS	-17.6983	-436.2698	-695.7	-693.4
HOCl	-19.8604	-536.0394	-680.0	-679.0
Atoms				
H	-1.3453	-0.5001		
Li	-2.9589	-7.4880		
F	-4.1183	-99.7712		
C	-3.8816	-37.8635		
O	-5.4419	-75.1031		
N	-6.2698	-54.6125		
P	-7.0574	-341.2900		
Si	-5.4910	-289.3931		
Cl	-6.0250	-460.1775		
S	-6.6058	-398.1421		

2. Effect of varying the amount of Fock exchange in PBE0 and B3LYP

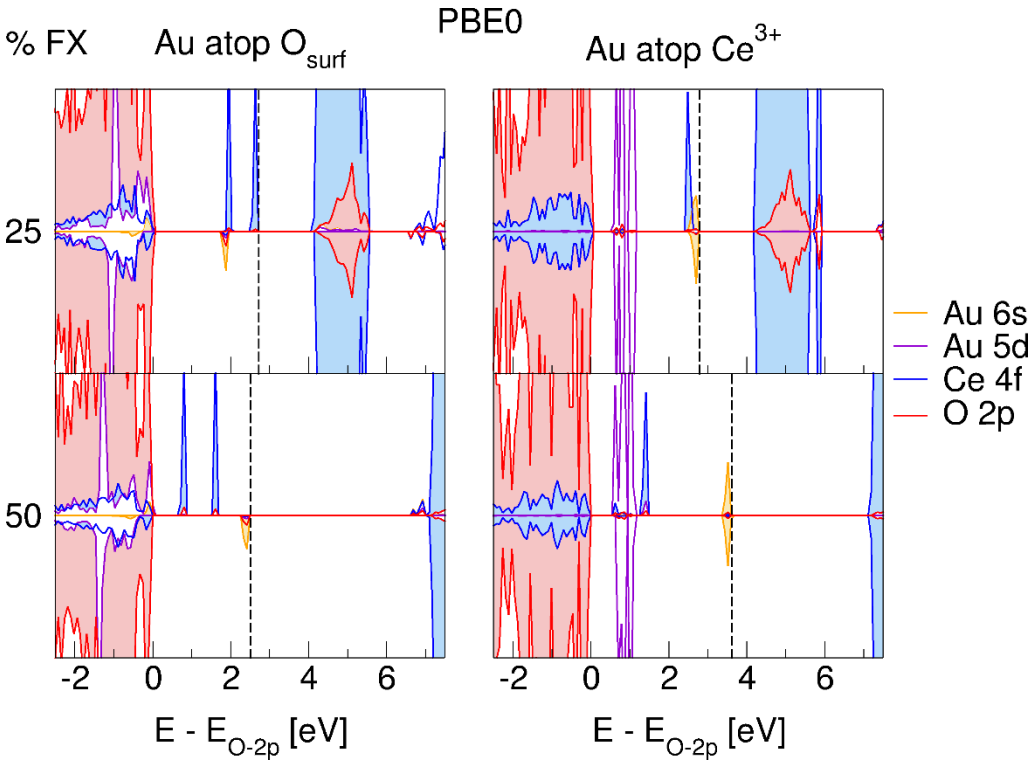

Figure S1 Orbitally projected DOS of Au adsorbed in atop position of O_{surf} (lhs) and atop Ce^{3+} (rhs) in the CeO_{2-x}(111) surface using PBE0 with 25% (top) and 50% (bottom) FX. The vertical dashed line indicates the highest occupied orbital energy.

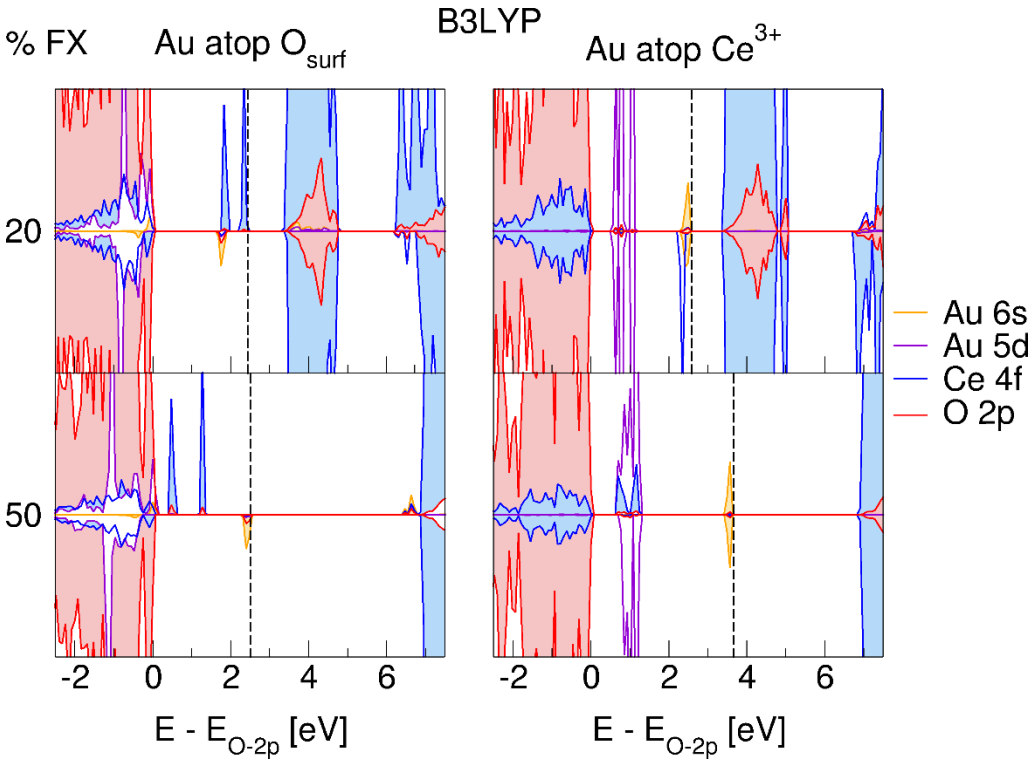

Figure S2 Orbitally projected DOS of Au adsorbed in atop position of O_{surf} (lhs) and atop Ce^{3+} (rhs) in the CeO_{2-x}(111) surface using B3LYP with 20% (top) and 50% (BHLYP, bottom) FX. The vertical dashed line indicates the highest occupied orbital energy.

3. Lattice parameters and bulk moduli of CeO_2

The lattice constants and bulk moduli of CeO_2 shown in Table S2 were calculated by performing seven single point calculations (= fixed cell volumes) centred around the minimum and by fitting the corresponding total energies to Murnaghan's equation of state.[2]

Table S2 Lattice constants a_0 and bulk moduli B_0 for various functionals.

	a_0 [Å]	B_0 [GPa]
Obsd.	5.41[a]	204-230[a]
LDA+U(5.3) [a]	5.40[a]	210[a]
PBE+U(4.5) [a]	5.49[a]	180[a]
HSE06	5.40[b]	207[b]
HSE03	5.40[a]	-
HSE(50% HF)	5.35	236
B3LYP	5.47[c]	190
BHLYP	5.42[c]	221
PBE0	5.39[a]	208
PBE0(50% HF)	5.35	237
TPSSh	5.42	196

[a] Ref. 3; [b] Ref. 4; [c] See also ref. 5.

4. Local magnetic moments

Table S3

Ce 4f	**Au@Ce^{3+}**	**Au@O^{2-}**		**Au@O_{sub}**
LDA+U	0.957	-0.964	-0.945	-0.969
PBE+U	0.962	-0.965	0.955	0.970
HSE	0.945	0.957	0.924	0.955
HSE (a_{FX} = 0.5)	0.974	0.972	0.970	0.972
PBE0	0.962	0.949	0.929	0.956
PBE0 (a_{FX} = 0.5)	0.973	0.970	0.971	0.969
B3LYP	0.957	0.942	0.902	0.951
BHLYP	0.975	0.972	0.972	0.971
TPSSh	0.792	0.859	0.700	0.834
TPSSh (a_F = 0.2)	0.944	0.949	0.866	-0.943
Au 6s				
LDA+U	-	0.199	-	-
PBE+U	-	0.221	-	-
HSE	-	-0.252	-	-
HSE (a_{FX} = 0.5)	-	0.276	-	-
PBE0	-	-0.256	-	-
PBE0 (a_{FX} = 0.5)	-	-0.279	-	-
B3LYP	-	-0.258	-	-
BHLYP	-	-0.288	-	-
TPSSh	-	-0.236	-	-
TPSSh (a_F = 0.2)	-	-0.253	-	-

Ce total	**Au@Ce^{3+}**	**Au@O^{2-}**		**Au@O_{sub}**
LDA+U	0.940	-0.947	-0.927	-0.951
PBE+U	0.930	-0.931	0.921	0.938
HSE	0.913	0.921	0.891	0.924
HSE (a_{FX} = 0.5)	0.939	0.941	0.934	0.939
PBE0	0.933	0.922	0.900	0.930
PBE0 (a_{FX} = 0.5)	0.950	0.945	0.946	0.946
B3LYP	0.928	0.915	0.874	0.925
BHLYP	0.953	0.949	0.950	0.950
TPSSh	0.762	0.824	0.677	0.816
TPSSh (a_F = 0.2)	0.905	0.909	0.835	-0.908
Au total				
LDA+U	-	0.359	-	-
PBE+U	-	0.378	-	-
HSE	-	-0.394	-	-
HSE (a_{FX} = 0.5)	-	0.396	-	-
PBE0	-	-0.392	-	-
PBE0 (a_{FX} = 0.5)	-	-0.398	-	-
B3LYP	-	-0.388	-	-
BHLYP	-	-0.403	-	-
TPSSh	-	-0.381		
TPSSh (a_F = 0.2)	-	-0.398	-	-

5. Calculated work functions

Table S4

cell size	DFA	CeO_2(111)	CeO_{2-x}(111) V_{surf}	CeO_{2-x}(111) V_{sub}	Au@V_{sub} atop Ce^{3+}	Au@V_{sub} atop O_{surf}	Au@V_{surf}
2x2	PBE+U	6.02	4.23	4.51	4.89	4.74	5.25
	HSE	7.14	4.07	4.13	4.97	4.62	4.88
4x4	PBE+U	6.00	4.82	4.86	4.64	4.69	5.06
	HSE	7.14		4.66			4.53

6. Relative stabilities of subsurface and surface Ce^{3+} in *p*(4 × 4)

Table S5 Relative energies in eV for surface and subsurface Ce^{3+} sites on the *p*(4 x 4) cell of CeO_2(111) with a single Na adatom.

Ce^{3+} site	LDA+*U*	PBE+*U*	HSE
surface	**0**	**0**	**0**
subsurface	+0.29	+0.10	+0.38

7. Computational details of *GW* calculations

Because of the increase in computational workload, we used a double trilayer CeO_2 model, i.e. a slab with composition Ce_8O_{15} (+ Au). The structure is identical to the optimized HSE structure of Au atop Ce^{3+} reported in the main text. HSE orbitals and orbital energies have been generated using 450 eV cutoff, 10^{-5} eV SCF break criterion, and a Γ-centred Monkhorst-Pack (4 × 4 × 1) k mesh. A Gaussian smearing together with a broadening of 0.02 eV was applied. They have been used as an input for G_0W_0 as well as GW_0 calculations.[6] The essential procedure follows the description presented on https://cms.mpi.univie.ac.at/vasp. Convergence of quasiparticle shifts has been carefully checked and reached using a total of 576 bands (involving 102 singly occupied bands for up-spin and 101 down-spin bands). Cutoff and smearing are identical to HSE calculations. The frequency grid uses 120 points, LMAXFOCKAE = 6, ENCUTGW = 150 eV, and the response function was evaluated using a reduced k grid (NKRED = 2) along periodic directions. GW_0 calculations use 4 iterations to update the Green's function.

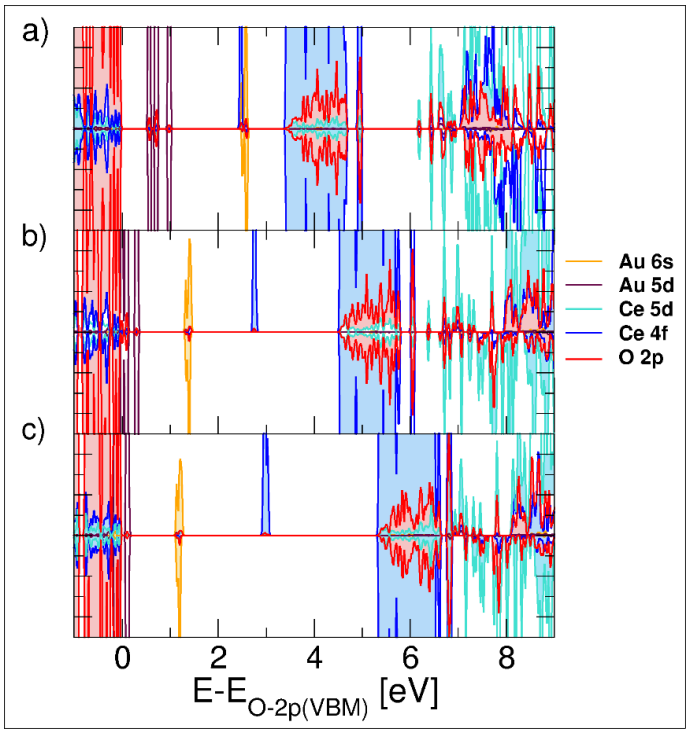

Figure S3 Orbitally projected density of states of Au atop Ce^{3+} calculated using a) HSE, b) G_0W_0(HSE), and c) GW_0(HSE).

8. Tests including the dispersion-correction after Grimme

The R_0 and C_6 parameters used are amply discussed in the Supplemental Information to reference [7]. The parameters for Au are discussed in reference [8].

Table S6 Adsorption energies (eV/Au atom). Values in parenthesis report the difference between corrected and uncorrected results.

	adsorption site	PBE+*U*+D2//PBE+*U*+D2[a]	HSE+D2//HSE+D2[a]
clean	O_{surf} atop	-1.27 (-0.20)	-0.66 (-0.18)
	O-O bridge	-1.38 (-0.18)	-0.59 (-0.28)
	O-Ce bridge	-1.00 (-0.21)	-0.68 (-0.16)
	Au_2 atop O_{surf}	-2.01 (-0.19)	-1.69 (-0.10)
reduced	O_{surf} atop	-1.01 (-0.23)	-0.74 (-0.19)
	O_{sub} atop	-1.22 (-0.27)	-1.17 (-0.22)
	Ce^{3+} atop	-0.88 (-0.24)	-0.84 (-0.20)

[a] Calculations use PBE+*U* and HSE lattice constants.

9. Total energies

Table S7 Total energies (eV) for the clean and the reduced CeO_{2-x}(111) surface.

			CeO_{2-x}(111)	
DFA	unit cell	CeO_2(111)	V_{surf}	V_{sub}
PBE+*U*	*p*(2 × 2)	-291.007208	-283.844502	-284.207031
	p(4 × 4)	-1164.038111	-1157.254144	-1157.354439
HSE	*p*(2 × 2)	-381.699813	-371.754632	-372.103672
	p(4 × 4)	-1526.694434	-1517.15814	-1517.30953

Table S8 Total energies (eV) for an isolated (gaseous) Au atom and the reduced CeO_{2-x}(111) surface (containing a subsurface O vacancy).

DFA	a_{FX}	CeO_{2-x}(111)	Au atom
LDA+*U*	0.00	-308.649789	-0.138733
PBE+*U*	0.00	-284.207031	-0.180984
HSE	0.25	-372.103672	-0.533293
	0.50	-450.315025	-0.921378
B3LYP	0.20	-364.278299	-0.609010
BHLYP	0.50	-481.354892	-1.367255
PBE0	0.25	-393.923283	-0.783079
	0.50	-494.123651	-1.460443
TPSSh	0.10	-463.560843	-0.510522

Table S9 Total energies (eV) for various adsorption sites in the *p*(2 × 2) cell of CeO_2(111) with one subsurface O vacancy corresponding to Table 1.

adsorption site	LDA+*U*	PBE+*U*	HSE
O_{surf} atop	-310.065113	-285.172367	-373.191200
O_{sub} atop	-310.639280	-285.335577	-373.590100
O-O bridge	[a]	-285.074008	-372.878069
V_{sub} atop	-310.419867	-284.936311	-372.543298
Ce^{4+} atop	-310.082775	-284.998289	-373.214142
Ce^{3+} atop	-310.084458	-285.032296	-373.276994

[a] Not stable; after optimization Au is in atop position of V_{sub}.

Table S10 Dependence of total energies (eV) on the $U_{Ce\text{-}4f}$ parameter in PBE+*U* calculations.

$U_{Ce\text{-}4f}$ (eV)	O_{surf} atop	Ce^{3+} atop
3.5	-288.643578	-288.730440
4.0	-286.881625	-286.865965
4.5	-285.172367	-285.032296
5.0	-283.500951	-283.290844

Table S11 Dependence of total energies (eV) on the $U_{Au\text{-}6s}$ parameter in PBE+*U* calculations.

	O_{surf} atop		Ce^{3+} atop	
$U_{Au\text{-}6s}$ (eV)	Au^0	$Au^{\delta+}$	Au^-	$Au^{\delta-}$
0.0	-285.172367	-285.033129	-285.032296	-285.023388
0.5	-285.049067		-284.929013	-284.879281
1.0	-284.961271		-284.788239	-284.754550
1.5	-284.861060	-284.732102	-284.685649	-284.670349
2.0	-284.758634	-284.621017	-284.541275	-284.594317
2.5	-284.665802		-284.425089	-284.469754
3.0	-284.570025		-284.317596	-284.380163
4.0	-284.378874		-284.065824	-284.210683
5.0	-284.205988		-283.842471	-284.036755
6.0	-284.025384		-283.607117	-283.878521

Table S12 Dependence of total energies (eV) on the $U_{Au\text{-}5d}$ parameter in PBE+*U* calculations.

	O_{surf} atop		Ce^{3+} atop	
$U_{Au\text{-}5d}$ (eV)	Au^0	$Au^{\delta+}$	Au^-	$Au^{\delta-}$
0.0	-285.172367	-285.033129	-285.032296	-285.023388
1.0	-284.680543	-284.536694	-284.554342	-284.531354
2.0	-284.234979	-284.107439	-284.101285	-284.143674
3.0	-283.861979		-283.696255	-283.760501
4.0	-283.537861	-283.417942	-283.334115	-283.474378
5.0	-283.264041		-283.055481	-283.235405
6.0	-283.104716		-282.854768	-283.055326
7.0	-283.064986			-283.022819

Table 13 Total energies (eV) for various adsorption sites in the *p*(2 × 2) cell of CeO_2(111) with one subsurface O vacancy corresponding to Table 4.

DFA	a_{FX}	O_{surf} atop	Ce^{3+} atop	O_{sub} atop
HSE	0.25	-373.191200	-373.276994	-373.590100
	0.50	-451.652642	-451.230206	-451.525324
B3LYP	0.20	-365.331270	-365.408832	-365.339543
BHLYP	0.50	-482.937287	-482.347873	-482.315254
PBE0	0.25	-395.230275	-395.324516	-395.614233
	0.50	-495.899286	-495.451133	-495.712073
TPSSh	0.10	-464.644337	-465.022960	-465.380324

Table S14 Total energies (eV) for surface and subsurface Ce^{3+} in the *p*(4 × 4) cell of CeO_2(111) doped with one Na adatom.

Ce^{3+} site	LDA+*U*	PBE+*U*	HSE
surface	-1149.990496	-1164.845882	-1681.396883
subsurface	-1150.068884	-1164.745304	-1680.936986

Table S15 Total energies (eV) for one Au atom and the vertical Au_2 dimer on the pristine CeO_2(111) surface.

DFA	site	*OS*(Au)	*p*(2 × 2)	*OS*(Au)	*p*(4 × 4)
PBE+*U*	O-O bridge	+1	-292.386513	+1	-1165.385193
	O_{surf} atop	+1	-292.262502	+1	-1165.280595
	O_{sub} atop	0	-291.800191	–	
	O_{sub} atop	+1	-292.238869	+1	-1165.147935
	O-Ce bridge	0	-291.978321	+1	-1165.048651
	Ce^{4+} atop	0	-291.583205	0	-1164.617978
	Au_2 atop O_{surf}	0	-295.025447	0	-1168.116070
HSE	O_{surf} atop	0	-382.709453	0	-1527.747151
	O-Ce bridge	0	-382.754703	0	-1527.733260
	O-O bridge	0	-382.545640	0	-1527.527978
	O-O bridge	+1	-382.658878	+1	-1527.743246
	Au_2 atop O_{surf}	0	-385.944070	0	

Table S16 Total energies (eV) for one Au atom and the vertical Au_2 dimer on the reduced CeO_{2-x}(111) surface.

DFA	site	*OS*(Au)	*p*(2 × 2)	site	*OS*(Au)	*p*(4 × 4)
PBE+*U*	O-O bridge	+1	-285.074008	O-O bridge	+1	-1158.683685
	O_{surf} atop	0	-285.172367	O_{surf} atop **a**	+1	-1158.393753
					0	-1158.396164
				O_{surf} atop **c**	+1	-1158.481315
	O_{sub} atop	-1	-285.335577	O_{sub} atop **d**	0	-1158.292444
	Ce^{3+} atop	-1	-285.032296	Ce^{3+} atop **1**	δ-	-1158.109342
	Ce^{4+} atop	-1	-284.998289			
	V_{surf} atop	-1	-286.461987	V_{surf} atop	-1	-1159.536010
	Au_2 atop V_{surf}	-1[a]	-287.611949	Au_2 atop V_{surf}	-1[a]	-1160.737073
HSE	O_{surf} atop	0	-373.191200	O_{surf} atop **a**	0	-1518.406380
				O_{surf} atop **b**	0	-1518.438724
				O_{surf} atop **c**	0	-1518.346473
	O_{sub} atop	-1	-373.590100	O_{sub} atop **d**	–	
	Ce^{3+} atop	-1	-373.276994	Ce^{3+} atop **1**	–	
	V_{surf} atop	-1	-374.758022	V_{surf} atop	-1	-1519.853420
	Au_2 atop V_{surf}	-1[a]	-376.100443			

[a] Oxidation state of the entire Au_2 dimer (Au_2^-).

References

1. G. Makov and M. C. Payne, *Phys. Rev. B*, 1995, **51**, 4014-4022.
2. F. D. Murnaghan, *Proc. Natl. Acad. Sci. U. S. A.*, 1944, **30**, 244-247.
3. J. L. F. Da Silva, M. V. Ganduglia-Pirovano, J. Sauer, V. Bayer and G. Kresse, *Phys. Rev. B*, 2007, **75**, 045121.
4. T. Kropp and J. Paier, *J. Phys. Chem. C*, 2014, **118**, 23690-23700.
5. J. Graciani, A. M. Marquez, J. J. Plata, Y. Ortega, N. C. Hernandez, A. Meyer, C. M. Zicovich-Wilson and J. F. Sanz, *J. Chem. Theory Comput.*, 2011, **7**, 56-65.
6. F. Fuchs, J. Furthmüller, F. Bechstedt, M. Shishkin and G. Kresse, *Phys. Rev. B*, 2007, **76**, 115109.
7. C. Penschke, J. Paier and J. Sauer, *J. Phys. Chem. C*, 2013, **117**, 5274-5285.
8. S. Tosoni, A. D. Boese and J. Sauer, *J. Phys. Chem. C*, 2011, **115**, 24871-24879.